

$\text{CBe}_5\text{H}_n^{n-4}$ ($n = 2-5$): Hydrogen-Stabilized CBe_5 Pentagons Containing Planar or Quasi-Planar Pentacoordinate Carbons

Jin-Chang Guo,^{*,†} Guang-Ming Ren,[†] Chang-Qing Miao,[†] Wen-Juan Tian,[‡] Yan-Bo Wu,^{*,‡} and Xiaotai Wang^{*,§}

[†]Institute of Materials Science and Department of Chemistry, Xinzhou Teachers' University, Xinzhou 034000, Shanxi, People's Republic of China

[‡]The Key Laboratory of the Materials for Energy Storage and Conversion of Shanxi Province, Institute of Molecular Science, Shanxi University, Taiyuan 030006, Shanxi, People's Republic of China

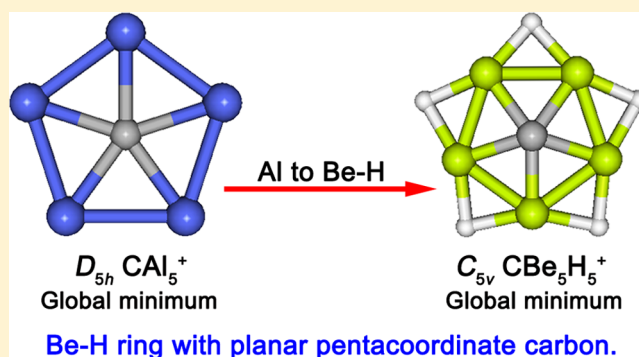
[§]Department of Chemistry, University of Colorado Denver, Campus Box 194, P.O. Box 173364, Denver, Colorado 80217-3364, United States

S Supporting Information

ABSTRACT: The diagonal relationship between beryllium and aluminum and the isoelectronic relationship between BeH unit and Al atom were utilized to design a new series ppC- or quasi-ppC-containing species $\text{C}_{5v} \text{CBe}_5\text{H}_5^+$, $\text{C}_s \text{CBe}_5\text{H}_4$, $\text{C}_{2v} \text{CBe}_5\text{H}_3^-$, and $\text{C}_{2v} \text{CBe}_5\text{H}_2^{2-}$ by replacing the Al atoms in previously reported global minima planar pentacoordinate carbon (ppC) species $D_{5h} \text{CAI}_5^+$, $\text{C}_{2v} \text{CAI}_4\text{Be}$, $\text{C}_{2v} \text{CAI}_3\text{Be}_2^-$, and $\text{C}_{2v} \text{CAI}_2\text{Be}_3^{2-}$ with BeH units. The three-center two-electron (3c-2e) bonds formed between Be and bridging H atoms were crucial for the stabilization of these ppC species.

The natural bond orbital (NBO) and adaptive natural density partitioning (AdNDP) analyses revealed that the central ppCs or quasi-ppCs possess the stable eight electron-shell structures.

The AdNDP analyses also disclosed that these species are all $6\sigma+2\pi$ double-aromatic in nature. The aromaticity was proved by the calculated negative nucleus-independent chemical shifts (NICS) values. DFT and high-level CCSD(T) calculations revealed that these ppC- or quasi-ppC species are the global minimum or competitive low-lying local minimum ($\text{C}_s \text{CBe}_5\text{H}_4$) on their potential energy surfaces. The Born–Oppenheimer molecular dynamic (BOMD) simulations revealed that the H atoms in $\text{C}_{2v} \text{CBe}_5\text{H}_3^-$ and $\text{C}_{2v} \text{CBe}_5\text{H}_2^{2-}$ can easily rotate around the CBe_5 cores and the structure of quasi-planar $\text{C}_{5v} \text{CBe}_5\text{H}_5^+$ will become the planar structure at room temperature; however, these interesting dynamic behaviors did not indicate the kinetic instability as the basic ppC structures were maintained during the simulations. Therefore, it would be potentially possible to realize these interesting ppC- or quasi-ppC-species in future experiments.



1. INTRODUCTION

In 1968, Monkhurst proposed the planar tetracoordinate carbon (ptC) geometry for the transition state describing the isomerization of a chiral molecule with a four-coordinate asymmetric carbon atom.¹ Two years later, through analyzing the electronic structure of planar methane, Hoffmann et al. proposed strategies for stabilizing ptC structures.² In 1976, the Schleyer and the Pople groups computationally characterized the first ptC molecule 1,1-dilithiumcyclopropane ($\text{C}_3\text{H}_4\text{Li}_2$).³ These seminal studies on ptC structures established the field of planar carbon chemistry, which has been growing and expanding to include planar penta-, hexa-, and heptacoordinate carbons.^{4–8} Experimentally, some ptC species have been observed and characterized in the gas phase, including CAI_4^- , NaCAI_4^- , CAI_3Si^- , CAI_3Ge^- , and C_2Al_4 .^{9–12}

In planar carbon chemistry, species with planar pentacoordinate and hexacoordinate carbons (ppC and phC) are particularly

interesting because of their structural diversity. In their 2001 groundbreaking work, Wang and Schleyer computed the first ppC structures, which they named “hyparenes.”¹³ They designed these hyparenes by replacing the $-(\text{CH})_3-$ subunits in aromatic and antiaromatic hydrocarbons using the borocarbon units $-\text{C}_3\text{B}_3-$, $-\text{C}_2\text{B}_4-$, and $-\text{CB}_5-$ with planar pentacoordinate carbons. In 2004, Li et al. demonstrated the possibility of hosting a ppC in the pentagonal copper hydride complex Cu_5H_5 .¹⁴ In 2008, Luo computed the smallest ppC-containing species CBe_5 and CBe_5^{4-} .¹⁵ In 2008, Zeng and Schleyer and colleagues reported the first global minimum structure containing a ppC, namely, the 18-electron $D_{5h} \text{CAI}_5^+$ (see 4 in Figure 1).¹⁶ Replacing the Al atom(s) in CAI_5^+ with Be atom(s) and

Received: October 17, 2015

Revised: December 4, 2015

Published: December 22, 2015

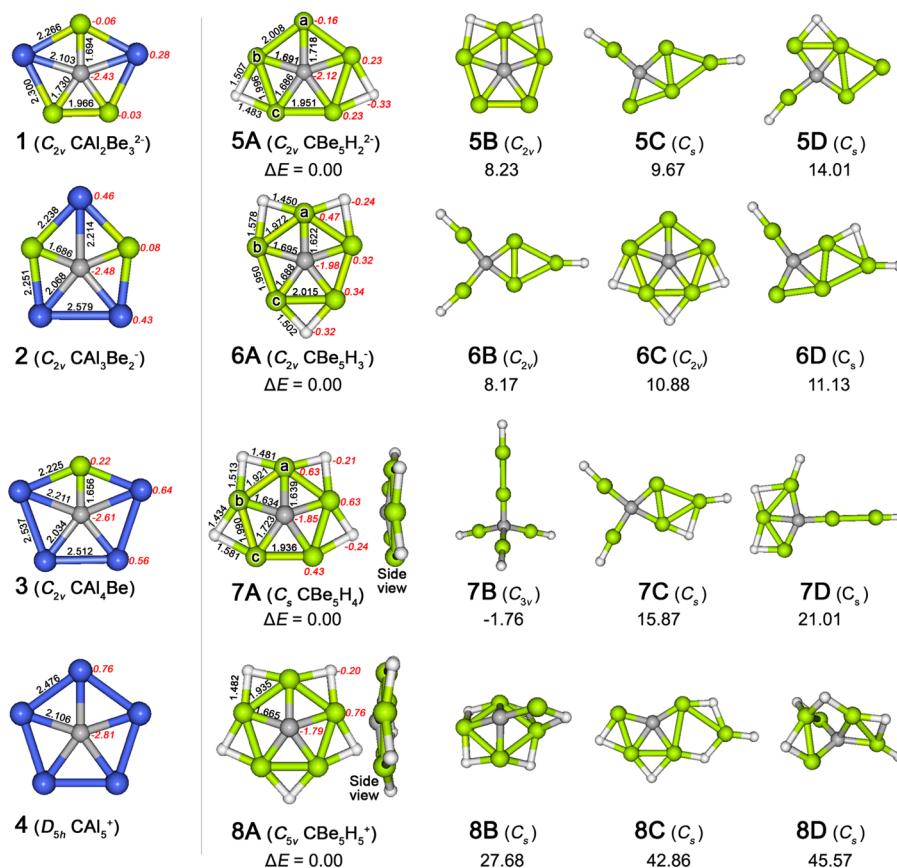


Figure 1. B3LYP/aug-cc-pVTZ optimized structures of 1–4, 5A–8A, and three lowest isomers of $CBe_5H_n^{n-4}$ ($n = 2-5$). The necessary bond lengths for 1–4 and 5A–8A are given in angstroms, the natural charges of 1–4 and 5A–8A are marked in red italic font, and the relative energies of $CBe_5H_n^{n-4}$ ($n = 2-5$) isomers are given in kilocalories per mole.

simultaneously retaining 18 valence electrons have led to more ppC global minima, including CaI_4Be , $CaI_3Be_2^-$, and $CaI_2Be_3^{2-}$ (see 1–3 in Figure 1).^{17,18} The ppC species stabilized by silicon were also reported.¹⁹ The first pHC D_{6h} CB_6^{2-} was reported in 2000 by the Schleyer group.²⁰ In 2007, using the strategy similar to design the hyparenes, Schleyer, Li, and coworkers designed a family of species with pHC.²¹ In 2008, the Zeng group explored the possibility of forming the ppC and pHC in binary boron-carbon clusters.²² Recently, our group proved that the pHC species D_{3h} $CO_3Li_3^+$ is the global minimum²³ and while pHC species D_{3h} $CN_3Be_3^+$ and D_{3h} $CN_3Mg_3^+$ are not the global minima, they possess the excellent kinetic stability, which would be feasible for experimental realization.²⁴

The present study focuses on the design of ppC species. Both the diagonal relationship between Al and Be and the isoelectronic relationship between Al and BeH were utilized to design new ppC or quasi-ppC species that are likely to be global minima, including C_{2v} $CBe_5H_2^{2-}$ (5A), C_{2v} $CBe_5H_3^-$ (6A), C_s CBe_5H_4 (7A), and C_{5v} $CBe_5H_5^+$ (8A). Note that 5A–8A are also isoelectronic with the recently reported $CBe_5Li_n^{n-4}$ series of ppC species.²⁵ The significance of this and the previous computational studies on the 18-electron global minimal ppC species is to provide experimentalists with potentially observable candidates.

2. COMPUTATIONAL METHODS

The potential energy surfaces of $CBe_5H_n^{n-4}$ ($n = 2-5$) were explored by the stochastic search algorithm, which was coded in the GXYZ program.²⁶ In our exploration, both singlet and triplet

surfaces were considered. The random structures generated by GXYZ were initially optimized at B3LYP/6-31G(d) level and then the ten lowest isomers found were reoptimized and the harmonic vibrational frequencies were analyzed at the B3LYP/aug-cc-pVTZ level.^{27–29} The energies of the isomers were further improved by the CCSD(T)/aug-cc-pVTZ^{30–32} single-point calculations based on the B3LYP/aug-cc-pVTZ optimized geometries. The relative energies of isomers were determined by the CCSD(T)/aug-cc-pVTZ energies plus the B3LYP/aug-cc-pVTZ zero-point energy corrections. Natural bond orbital (NBO) and adaptive nature density partitioning (AdNDP) analyses^{33,34} were performed at B3LYP/aug-cc-pVTZ and B3LYP/6-31G levels, respectively, to gain insight into the bonding characters of these species. The nucleus-independent chemical shifts (NICS)^{35–37} were calculated at the centers of the three-membered rings and the points located 1 Å above the centers of the three-membered rings and above the ppCs/quasi-ppCs to assess the aromatic nature of these ppC species. The vertical detachment energies (VDEs) for $CBe_5H_n^{n-4}$ ($n = 2-5$) and the vertical electron affinities (VEAs) for $CBe_5H_5^+$ were calculated with the outer valence Green's function (OVGF).³⁸ All calculations in this work were performed using the Gaussian 09 package.³⁹ Molecular structures and AdNDP partitioned orbitals were visualized using the Molekel 5.4 program.⁴⁰

3. RESULTS AND DISCUSSION

3.1. Design and Characterization of $CBe_5H_n^{n-4}$ ($n = 2-5$). The optimized structures of 1–4 are shown in Figure 1.

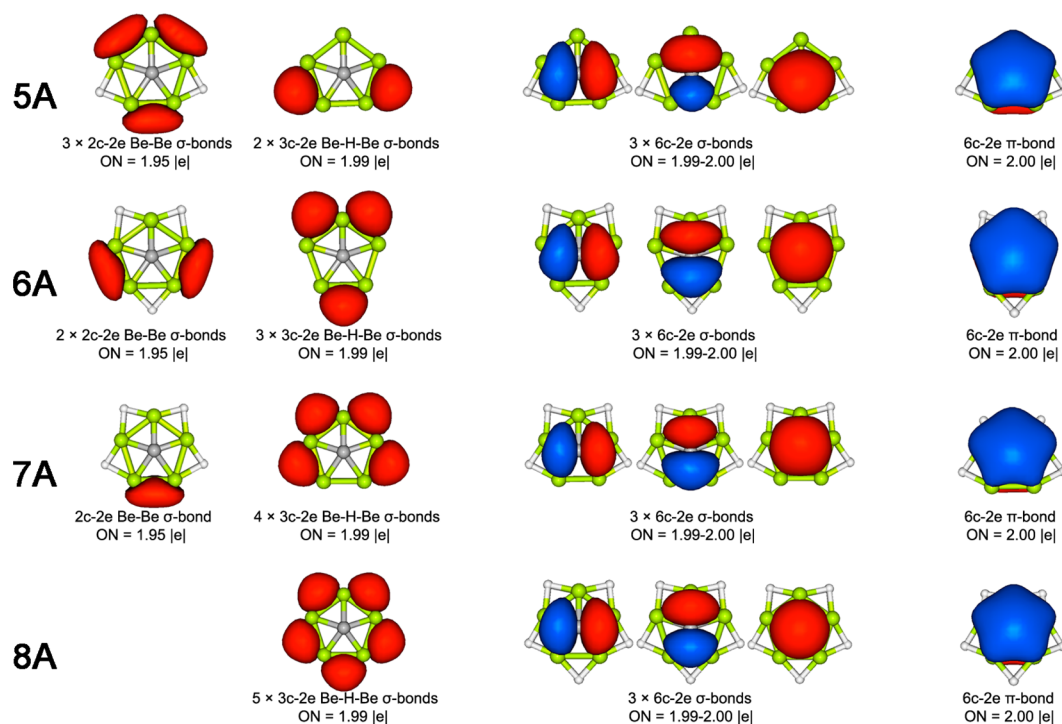


Figure 2. AdNDP analyses results of 5A–8A.

Table 1. Lowest Vibrational Frequencies ($\nu_{\text{min}}/\text{cm}^{-1}$), HOMO-LUMO Gaps (Gap/eV), and Wiberg Bond Indices (WBI) of the C–Be, Be–Be, Be–H Bonds, and Total WBIs of C, Be, and H Atoms of $\text{CBe}_5\text{H}_n^{n-4}$ ($n = 2-5$) at the B3LYP/aug-cc-pVTZ Level

	ν_{Min}	Gap	WBI _{C-Be}		WBI _{Be-Be}		WBI _{Be-H}		WBI _{Be}		WBI _H
			Be _a /Be _b /Be _c	a-b/b-c/c-c ^a	Be _a /Be _b /Be _c	WBI _C	Be _a /Be _b /Be _c	ab/bc/cc ^b			
$\text{CBe}_5\text{H}_2^{2-}$	221	0.76	0.48/0.58/0.61	0.92/0.18/0.93	---/0.42/0.46	2.88	2.58/2.29/2.39	---/0.91/---			
CBe_5H_3^-	162	2.23	0.77/0.55/0.55	0.20/0.96/0.16	0.56/0.35/0.44	2.99	2.42/2.19/2.25	0.95/---/0.92			
CBe_5H_4	125	2.60	0.72/0.69/0.48	0.23/0.18/0.96	0.48/0.45/-----/0.57/0.35	3.09	2.24/2.22/2.07	0.97/0.95/---			
CBe_5H_5^+	173	6.09	0.62	0.22	0.46	3.15	2.05	0.97			

^a“a-b”, “b-c”, and “c-c” denote Be_a-Be_b, Be_b-Be_c, and Be_c-Be_c. “a”, “b”, and “c” correspond the numbering of Be atoms of 5A, 6A, and 7A in Figure 1. ^b“ab”, “bc”, and “cc” denote the positions where the bridge H atoms locate. “a”, “b”, and “c” correspond the numbering of Be atoms of 5A, 6A, and 7A in Figure 1.

To design the new ppC species, we replaced all aluminum atoms in 1–4 with Be atoms and attached corresponding number of H atoms to these Be atoms. According to the different position of H atoms, two types of structures were considered, one with the terminal-H (H atoms attach to Be vertexes) and the other with the bridging-H (H atoms attach to Be–Be edges). The calculations at B3LYP/aug-cc-pVTZ level revealed high preference of the bridging-H. For $\text{CBe}_5\text{H}_2^{2-}$ with terminal H, its structure will be converted to that with bridging-H. For the CBe_5H_3^- , CBe_5H_4 , and CBe_5H_5^+ , the structures with terminal-H are not minima and the vectors of smallest vibrational frequencies correspond to the counter-rotation between the H atoms and the CBe_5 cores, showing the inherent trend of the structural transition to geometry the bridging-H atom. As expected, at the B3LYP/aug-cc-pVT level, the planar structures for $\text{CBe}_5\text{H}_2^{2-}$ and CBe_5H_3^- with the bridging-H atoms (see 5A and 6A in Figure 1) are energy minima and although the planar structures for CBe_5H_4 and CBe_5H_5^+ are the first-order saddle points, releasing the geometrical strains according to the vectors of the imaginary frequency leads to the quasi-planar structures that maintain the basic ppC arrangements (the ppC atoms located only 0.18 and 0.25 Å above the Be₅ planes in 7A

and 8A, respectively; see Figure 1). Thermodynamically, the structures with bridging-H are 44.4, 33.6, and 123.4 kcal/mol lower in energy than those with terminal-H for CBe_5H_3^- , CBe_5H_4 , and CBe_5H_5^+ , respectively. Thus, our attentions were paid to the structures with the bridging-H atoms in the following.

To better understand the chemical bonding in 5A–8A, we performed the AdNDP analyses and the results are given in Figure 2. As the first column of the Figure shows, for the Be–Be edges without H atom, there has a 2c-2e Be–Be σ -bond with occupation numbers (ONs) of 1.95 |e|, while for those with H atom (see the second column in Figure 2), there is a 3c-2e Be–H–Be bond with the ONs of 1.99 |e|. Going from 5A to 8A, the number of 3c-2e Be–H–Be bonds increases from two to five and the gaps between the highest occupied molecular orbitals (HOMO) and the lowest unoccupied molecular orbitals (LUMOs) (see Table 1) increase from 0.76 to 2.23, 2.60, and 6.09 eV at the B3LYP/aug-cc-pVTZ level. The HOMO–LUMO gap for 8A (6.09 eV) is obviously larger than that for other species, indicating the good stability. The formation of 3c-2e Be–H–Be bonds should be a factor for the stabilization of these ppC or quasi-ppC species. The remained orbitals are almost identical for 5A–8A: The orbitals in the third to fifth columns are

delocalized 6c-2e σ bonds (ON = 1.99–2.00 |el) and those in last column are 6c-2e π bonds (ON = 2.00 |el). These four orbitals form the stable eight electrons shell structure for center carbon atoms in each of 5A–8A, which would be a reason why the ppC or quasi-ppC can be stabilized.

In addition to offering the stable shell structure for carbon, these four orbitals also contribute to the aromaticity: Three delocalized σ orbitals and one delocalized π orbitals match the Huckel's $4n + 2$ aromatic rule where $n = 1$ and 0, and thus 5A–8A are σ and π double-aromatic in nature. The aromaticity can be further confirmed by the NICS calculations on the concerned points, including the centers of the three-membered rings and the points located 1 Å above the centers of the three-membered rings and above the ppCs/quasi-ppCs. As shown in Figure 3, the

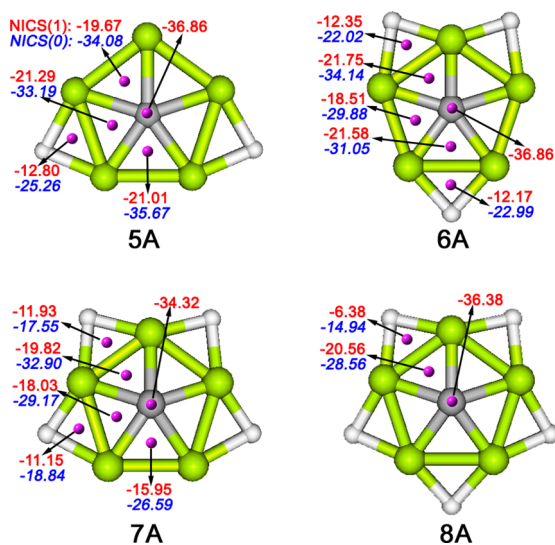


Figure 3. Positions and corresponding NICS values of 5A–8A. The NICS(1) values are marked in normal red font and the NICS(0) values are marked in italic blue font.

B3LYP/aug-cc-pVTZ calculated NICS(0) and NICS(1) values at all points are largely negative, suggesting that 5A–8A are aromatic in nature. This is consistent with the above the orbital analysis results. The aromaticity contributes to the stabilization of ppC in 5A–8A.

Electronically, 5A–8A are also isoelectronic to the previously reported CBe_5^{4-} molecule, and they can be considered as the molecules obtained by attaching certain number of H^+ cations to CBe_5^{4-} . In comparison with attaching Li^+ cations, which leads to positive–positive–negative (Li–Be–C) charge distribution in $\text{CBe}_5\text{Li}_n^{n-4}$ ($n = 2-5$), the NBO analysis suggest the natural charges for H, Be, and C atoms in 5A–8A are $-0.20 \sim -0.32$, $0.23-0.76$, and $-1.79 \sim -2.12$ |el, respectively, showing the obvious sandwich-type negative–positive–negative charge distribution. The attractive H–Be and Be–C electrostatic interactions in 5A–8A would be better than the attractive Be–C but repulsive Li–Be electrostatic interactions in $\text{CBe}_5\text{Li}_n^{n-4}$ ($n = 2-5$). The Wiberg bond orders of C–Be bond ($\text{WBI}_{\text{C-Be}}$) in species 5A–8A range from 0.48 to 0.77, suggesting significant covalent property. With regard to the Be–Be bonding, there are two types of Be–Be bonds, that is, with or without bridging H atom. For those without H atoms, the $\text{WBI}_{\text{Be-Be}}$ values in 5A–7A range from 0.92 to 0.96, suggesting the typical single bond; for those with bridging H atoms, the $\text{WBI}_{\text{Be-Be}}$ values are very small, ranging from 0.16 to 0.22. However, this is not the result of

weakened covalent interactions in 5A–8A but that of the formation of Be–H–Be three-center two-electron (3c-2e) bonds, which can be proved by the sum of $\text{WBI}_{\text{Be-H}}$ values of 0.88 to 0.92 for each H atom. The total Wiberg bond indices for C, Be, and H (WBI_{C} , WBI_{Be} , and WBI_{H}) range from 2.88, 2.05, and 0.91 to 3.15, 2.58, and 0.97, respectively. The doubled WBI_{C} values plus the natural charges on C are 7.88, 7.96, 8.03, and 7.99 for 5A–8A, respectively, revealing the stable eight-electron shell structure for carbon atoms. The WBI_{Be} values are larger than 2.00, which would be the results of the multiple center bonding around the Be atoms.

3.2. Stability Consideration. In the next, we study the stabilities of 5A–8A, which are crucial for their possibility to be realized. The thermodynamic stability is explored by the stochastic search algorithm. As shown in Figure 1, with the consideration of B3LYP/aug-cc-pVTZ zero-point energy (ZPE), the CCSD(T)/aug-cc-pVTZ calculations rank 5A, 6A, and 8A, the global minima on $\text{CBe}_5\text{H}_2^{2-}$, CBe_5H_3^- , and CBe_5H_5^+ potential energy surfaces, which are 8.23, 8.17, and 27.68 kcal/mol lower than corresponding second lowest isomers 5B, 6B, and 8B, respectively. Although 7A is the second lowest isomer, it is only 1.76 kcal/mol higher than corresponding global minimum 7B with a classical tetrahedral carbon, it should also be competitive in the experiments. The good thermodynamic stability of 5A–8A will benefit their generation in the gas-phase synthesis.

The kinetic stability is equally important for the experimental realization. We studied the kinetic stability of 5A–8A by running 100 ps adiabatic BOMD simulations at B3LYP/6-31G(d) level at 298 K. The root-mean-square deviations (RMSD, relative to the B3LYP/6-31G(d) optimized structures) of the structures are given in Figure 4. As the Figure 4 shows, the RMSD curve of 5A (first row in Figure 4) is most complicated and is also most interesting. It has six sharp jumps at approximately 38, 45, 65, 77, 90, and 93 ps, respectively, which reveal six times of isomerization. Remarkably, the magnitude for the fluctuation of the RMSD curve does not change after each jump, suggesting that the potential energies of these isomers are almost the same. Why did the potential energies not obviously change after the isomerization? The detailed structural sampling can answer this question. We found that the isomerization corresponds to the rotation of two H atoms around the CBe_5 core (see the first row in Figure 4), which revealed that the position of H atoms is highly flexible in 5A. The flexibility of H atoms in 6A is lower than that in 5A. As shown in the second row in Figure 4, there is only one jump of RMSD curve (at 91 ps) during the 100 ps simulations. Similar to the situation in the simulation of 5A, the isomerization also corresponds to the change of position of a H to a different Be–Be edge. The RMSD curves for the simulation of 7A and 8A have no sharp jump (the third and fourth row of Figure 4), indicating that their original structures are maintained very well during the 100 ps simulations. Despite the increasing flexibility of H atoms with the decreased number of H atoms in 5A–8A, the dynamic behaviors suggest that they are kinetically stable.

Notably, the RMSD curve for 8A can be divided into two parts. The curve before 56 ps had the similar appearance to those of other simulations when a structure is continuously maintained, but that after 56 ps had a different appearance, which attracted our special attention. We run the BOMD simulation of 8A for the second time, but the RMSD curves had the similar curve type change at 32 ps. We carefully checked the structure and found that before the curve-type changes the carbon atom and hydrogen atoms are located obviously out of the approximate plane defined by five Be atoms. In contrast, despite the thermal

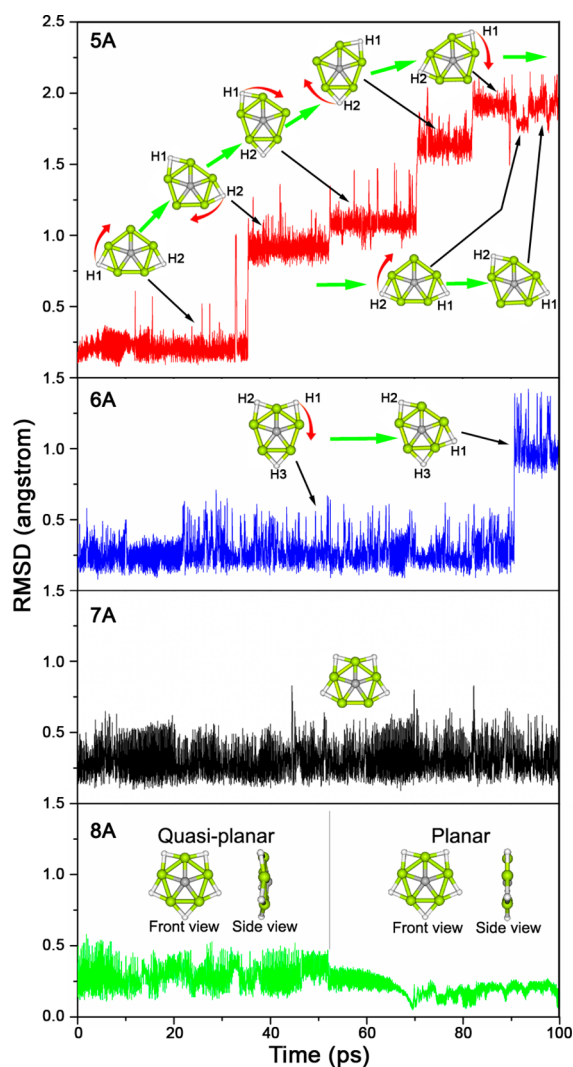


Figure 4. RMSD versus time for the BOMD simulations of 5A–8A at 298 K.

vibrations, all atoms are almost in the same plane after the curve-type changes. (See the movie in the Supporting Information for the sample of structures near 69 ps.) Therefore, we can easily understand the curve-type changes: According to static structural optimizations, the planar structure is first-order saddle point and a little higher in energy than the nonplanar minimum, and thus because of the adiabatic simulation manner, when the structure is changed from nonplanar to planar, the increased potential energy will certainly be accompanied by decreased kinetic energy, which will decrease the magnitude of the thermal vibrations and thus will decrease the fluctuation of the RMSD curve.

3.3. Vertical Detachment Energies and Electron Affinities. Because 5A–8A are global minima or competitive low-lying local minimum with good kinetic stability, it may be possible to detect them in the gas-phase experiments. Here we calculate the VDEs and the VEAs at OVGf/aug-cc-pVTZ to aid the possible future experimental confirmation. The anionic species 5A and 6A have the VDE values of -1.48 and 2.03 eV with the pole strengths of 0.86 and 0.88 , respectively. The negative VDE values for 5A suggest that its electrons will be autodetached and thus 5A may only be detected as cation-stabilized salt-like compound(s). The neutral species 7A has the VDE value of 6.29 eV with pole strengths of 0.89 . The cationic

species 8A has the VDE and VEA values of 14.46 and 4.13 eV with pole strength of 0.90 and 0.95 , respectively. This VEA value is similar to that of K^+ (4.1 eV), which, together with the extremely excellent thermodynamic and kinetic stabilities and the very large HOMO–LUMO gap (being 11.08 eV at MP2/aug-cc-pVTZ level), suggest that it can be considered as a pseudoalkali metal cation.

4. SUMMARY

In summary, we have proved that it is possible to replace the Al atoms in previously reported ppC-containing global minima D_{5h} CaI_5^+ , C_{2v} CaI_4Be , C_{2v} $CaI_3Be_2^-$, and C_{2v} $CaI_2Be_3^{2-}$, with the isoelectronic BeH groups to design the new ppC- or quasi-ppC species $CBe_5H_n^{n-4}$ ($n = 2-5$). Three factors, including the formation of peripheral $3c-2e$ Be–H–Be bond, the formation of the stable eight-electron shell structure for the central ppCs or quasi-ppCs and the $6\sigma+2\pi$ double aromaticity, contribute to the stabilization of ppC- or quasi-ppC-containing structures in $CBe_5H_n^{n-4}$ ($n = 2-5$) species. According to our extensive exploration of the potential energy surfaces, these species are the global minimum or competitive low-lying local minimum. The dynamic simulations revealed their interesting kinetic behaviors and also the very good kinetic stabilities. These ppC or quasi-ppC species would be targeted in future experiments.

■ ASSOCIATED CONTENT

Supporting Information

The Supporting Information is available free of charge on the ACS Publications website at DOI: [10.1021/acs.jpca.5b10178](https://doi.org/10.1021/acs.jpca.5b10178).

Video recording the samples of $CBe_5H_5^+$ structures during the dynamic simulation. (AVI)

Cartesian coordinates, the lowest vibrational frequencies ($\nu_{\min}/\text{cm}^{-1}$), and total energies (including zero-point energy (ZPE) corrections) of 1–4, 5A–8A, and the lowest three isomers of 5A–8A at B3LYP/aug-cc-pVTZ level and the ZPE-corrected CCSD(T)/aug-cc-pVTZ energies of 5A–8A and their isomers. (PDF)

■ AUTHOR INFORMATION

Corresponding Authors

*J.-C.G.: E-mail: gjchang01@yahoo.com. Tel: +86 350 333 9205.

*Y.-B.W.: E-mail: wyb@sxu.edu.cn. Tel: +86 351 701 8113.

*X.W.: E-mail: xiaotai.wang@ucdenver.edu. Tel: (303) 556 6711.

Notes

The authors declare no competing financial interest.

■ ACKNOWLEDGMENTS

This work was supported financially by National Natural Science Foundation of China (grant nos. 21003086, 21273140, and 21471092), the Shanxi Natural Science Foundation (2012021007-3), and the Program for the Innovative Talents of Higher Learning Institutions of Shanxi Province.

■ REFERENCES

- (1) Monkhorst, H. J. Activation Energy for Interconversion of Enantiomers Containing an Asymmetric Carbon Atom without Breaking Bonds. *Chem. Commun.* **1968**, 1111–1112.
- (2) Hoffmann, R.; Alder, R. W.; Wilcox, C. F., Jr Planar Tetracoordinate Carbon. *J. Am. Chem. Soc.* **1970**, *92*, 4992–4993.
- (3) Collins, J. B.; Dill, J. D.; Jemmis, E. D.; Apeloig, Y.; Schleyer, P. v. R.; Seeger, R.; Pople, J. A. Stabilization of Planar Tetracoordinate Carbon. *J. Am. Chem. Soc.* **1976**, *98*, 5419–5427.

- (4) Sorger, K.; von Rague Schleyer, P. Planar and Inherently Non-tetrahedral Tetracoordinate Carbon: A Status Report. *J. Mol. Struct.: THEOCHEM* **1995**, *338*, 317–346.
- (5) Minkin, V. I.; Minyaev, R. M.; Hoffmann, R. Non-Classical Structures of Organic Compounds: Unusual Stereochemistry and Hypercoordination. *Russ. Chem. Rev.* **2002**, *71*, 869–892.
- (6) Keese, R. Carbon Flatland: Planar Tetracoordinate Carbon and Fenestranes. *Chem. Rev.* **2006**, *106*, 4787–4808.
- (7) Merino, G.; Mendez-Rojas, M. A.; Vela, A.; Heine, T. Recent Advances in Planar Tetracoordinate Carbon Chemistry. *J. Comput. Chem.* **2007**, *28*, 362–372.
- (8) Yang, L. M.; Ganz, E.; Chen, Z. F.; Wang, Z. X.; Schleyer, P. v. R. Four Decades of the Chemistry of Planar Hypercoordinate Compounds. *Angew. Chem., Int. Ed.* **2015**, *54*, 9468–9501.
- (9) Li, X.; Wang, L. S.; Boldyrev, A. I.; Simons, J. Tetracoordinated Planar Carbon in the Al_4C^- anion: A Combined Photoelectron Spectroscopy and ab initio Study. *J. Am. Chem. Soc.* **1999**, *121*, 6033–6038.
- (10) Li, X.; Zhang, H. F.; Wang, L. S.; Geske, G. D.; Boldyrev, A. I. Pentaatomic Tetracoordinate Planar Carbon, $[CAL_4]^{2-}$: A New Structural Unit and Its Salt Complexes. *Angew. Chem., Int. Ed.* **2000**, *39*, 3630–3632.
- (11) Wang, L. S.; Boldyrev, A. I.; Li, X.; Simons, J. Experimental Observation of Pentaatomic Tetracoordinate Planar Carbon-Containing Molecules. *J. Am. Chem. Soc.* **2000**, *122*, 7681–7687.
- (12) Boldyrev, A. I.; Wang, L. S. Beyond Classical Stoichiometry: Experiment and Theory. *J. Phys. Chem. A* **2001**, *105*, 10759–10775.
- (13) Wang, Z. X.; Schleyer, P. v. R. Construction Principles of "Hyparenes": Families of Molecules with Planar Pentacoordinate Carbons. *Science* **2001**, *292*, 2465–2469.
- (14) Li, S. D.; Miao, C. Q.; Ren, G. M. D_{3h} Cu_5H_5X : Pentagonal Hydrocopper Cu_5H_5 Containing Pentacoordinate Planar Nonmetal Centers ($X = B, C, N, O$). *Eur. J. Inorg. Chem.* **2004**, *2004*, 2232–2234.
- (15) Luo, Q. Theoretical Observation of Hexaatomic Molecules Containing Pentacoordinate Planar Carbon. *Sci. China, Ser. B: Chem.* **2008**, *51*, 1030–1035.
- (16) Pei, Y.; An, W.; Ito, K.; Schleyer, P. v. R.; Zeng, X. C. Planar Pentacoordinate Carbon in Ca_3^+ : A Global Minimum. *J. Am. Chem. Soc.* **2008**, *130*, 10394–10400.
- (17) Jimenez-Halla, J. O. C.; Wu, Y.-B.; Wang, Z.-X.; Islas, R.; Heine, T.; Merino, G. Ca_4Be and $Ca_3Be_2^-$: Global Minima with A Planar Pentacoordinate Carbon Atom. *Chem. Commun.* **2009**, *46*, 8776–8778.
- (18) Wu, Y. B.; Duan, Y.; Lu, H. G.; Li, S. D. $Ca_2Be_3^{2-}$ and Its Salt Complex $Li Ca_2Be_3^-$: Anionic Global Minima with Planar Pentacoordinate Carbon. *J. Phys. Chem. A* **2012**, *116*, 3290–3294.
- (19) Zdetsis, A. D. Novel Pentagonal Silicon Rings and Nanowheels Stabilized by Flat Pentacoordinate Carbon(s). *J. Chem. Phys.* **2011**, *134*, 094312(1–5).
- (20) Exner, K.; Schleyer, P. v. R. Planar hexacoordinate carbon: A viable possibility. *Science* **2000**, *290*, 1937–1940.
- (21) Ito, K.; Chen, Z. F.; Corminboeuf, C.; Wannere, C. S.; Zhang, X. H.; Li, Q. S.; Schleyer, P. v. R. Myriad planar hexacoordinate carbon molecules inviting synthesis. *J. Am. Chem. Soc.* **2007**, *129*, 1510–1511.
- (22) Pei, Y.; Zeng, X. C. Probing the Planar Tetra-, Penta-, and Hexacoordinate Carbon in Carbon–Boron Mixed Clusters. *J. Am. Chem. Soc.* **2008**, *130*, 2580–2592.
- (23) Wu, Y. B.; Duan, Y.; Lu, H. G.; Lu, H. G.; Yang, P.; Schleyer, P. v. R.; Merino, G.; Islas, R.; Wang, Z. X. D_{3h} $CN_3Be_3^+$ and $CO_3Li_3^+$: viable planar hexacoordinate carbon prototypes. *Phys. Chem. Chem. Phys.* **2012**, *14*, 14760–14763.
- (24) Zhang, C. F.; Han, S. J.; Wu, Y. B.; Lu, H. G.; Lu, G. Thermodynamic Stability versus Kinetic Stability: Is the Planar Hexacoordinate Carbon Species D_{3h} $CN_3Mg_3^+$ Viable? *J. Phys. Chem. A* **2014**, *118*, 3319–3325.
- (25) Grande-Aztatzi, R.; Cabellos, J. L.; Islas, R.; Infante, I.; Mercero, J. M.; Restrepo, A.; Merino, G. Planar Pentacoordinate Carbons in CBe_5^+ Derivatives. *Phys. Chem. Chem. Phys.* **2015**, *17*, 4620–4624.
- (26) Lu, H. G.; Wu, Y. B. GXYZ; Shanxi University: Taiyuan, China, 2008.
- (27) Becke, A. D. Density Functional Thermochemistry. III. The Role of Exact Exchange. *J. Chem. Phys.* **1993**, *98*, 5648–5659.
- (28) Lee, C.; Yang, W.; Parr, R. G. Development of the Colle-Salvetti Correlation-Energy Formula into A Functional of the Electron Density. *Phys. Rev. B: Condens. Matter Mater. Phys.* **1988**, *37*, 785–791.
- (29) Kendall, R. A.; Dunning, T. H.; Harrison, R. J. Electron Affinities of the First-Row Atoms Revisited. Systematic Basis Sets and Wave Functions. *J. Chem. Phys.* **1992**, *96*, 6796–6806.
- (30) Pople, J. A.; Head-Gordon, M.; Raghavachari, K. Quadratic Configuration Interaction. A General Technique for Determining Electron Correlation Energies. *J. Chem. Phys.* **1987**, *87*, 5968–5975.
- (31) Scuseria, G. E.; Schaefer, H. F., III Is Coupled Cluster Singles and Doubles (CCSD) more Computationally Intensive than Quadratic Configuration Interaction (QCISD)? *J. Chem. Phys.* **1989**, *90*, 3700–3703.
- (32) Scuseria, G. E.; Janssen, C. L.; Schaefer, H. F., III An Efficient Reformulation of the Closed-shell Coupled Cluster Single and Double Excitation (CCSD) Equations. *J. Chem. Phys.* **1988**, *89*, 7382–7387.
- (33) Zubarev, D. Y.; Boldyrev, A. I. Developing Paradigms of Chemical Bonding: Adaptive Natural Density Partitioning. *Phys. Chem. Chem. Phys.* **2008**, *10*, 5207–5217.
- (34) Zubarev, D. Y.; Boldyrev, A. I. Revealing Intuitively Assessable Chemical Bonding Patterns in Organic Aromatic Molecules via Adaptive Natural Density Partitioning. *J. Org. Chem.* **2008**, *73*, 9251–9258.
- (35) Schleyer, P. v. R.; Maerker, C.; Dransfeld, A.; Jiao, H.; Hommes, N. J. R. E. Nucleus-Independent Chemical Shifts: A Simple and Efficient Aromaticity Probe. *J. Am. Chem. Soc.* **1996**, *118*, 6317–6318.
- (36) Schleyer, P. v. R.; Jiao, H.; Hommes, N. J. R. E.; Malkin, V. G.; Malkina, O. L. An Evaluation of the Aromaticity of Inorganic Rings: Refined Evidence from Magnetic Properties. *J. Am. Chem. Soc.* **1997**, *119*, 12669–12670.
- (37) Corminboeuf, C.; Heine, T.; Seifert, G.; von Rague Schleyer, P. v. R.; Weber, J. Induced Magnetic Fields in Aromatic [n]-Annulenes-Interpretation of NICS Tensor Components. *Phys. Chem. Chem. Phys.* **2004**, *6*, 273–276.
- (38) Ortiz, J. V. Toward an Exact One-Electron Picture of Chemical Bonding. *Adv. Quantum Chem.* **1999**, *35*, 33–52.
- (39) Frisch, M. J.; Trucks, G. W.; Schlegel, H. B.; Scuseria, G. E.; Robb, M. A.; Cheeseman, J. R.; Scalmani, G.; Barone, V.; Mennucci, B.; Petersson, G. A. et al. *Gaussian 09*, Revision A02; Gaussian, Inc.: Wallingford, CT, 2009.
- (40) Varetto, U. *Molekel*, version 5.4.0.8; Swiss National Supercomputing Centre: Manno, Switzerland, 2009.